

## Phase Transitions in Solids Stimulated by Simultaneous Exposure to High Pressure and Relativistic Heavy Ions

Ulrich A. Glasmacher,<sup>1,\*†</sup> Maik Lang,<sup>2</sup> Hans Keppler,<sup>3</sup> Falko Langenhorst,<sup>4</sup> Reinhard Neumann,<sup>2</sup> Dieter Schardt,<sup>2</sup> Christina Trautmann,<sup>2</sup> and Günther A. Wagner<sup>1,5</sup>

<sup>1</sup>*Forschungsstelle Archäometrie der Heidelberger Akademie der Wissenschaften am Max-Planck-Institut für Kernphysik, Saupfercheckweg 1, 69029 Heidelberg, Germany*

<sup>2</sup>*Gesellschaft für Schwerionenforschung (GSI), Planckstraße 1, 64291 Darmstadt, Germany*

<sup>3</sup>*Bayerisches Geoinstitut, Universität Bayreuth, Universitätsstraße 30, 95440 Bayreuth, Germany*

<sup>4</sup>*Institut für Geowissenschaften, Friedrich-Schiller-Universität, Burgweg 11, 07749 Jena, Germany*

<sup>5</sup>*Max-Planck-Institut für Kernphysik, Saupfercheckweg 1, 69029 Heidelberg, Germany*

(Received 9 November 2005; revised manuscript received 28 March 2006; published 17 May 2006)

In many solids, heavy ions of high kinetic energy (MeV-GeV) produce long cylindrical damage trails with diameters of order 10 nm. Up to now, no information was available how solids cope with the simultaneous exposure to these energetic projectiles and to high pressure. We report the first experiments where relativistic uranium and gold ions from the SIS heavy-ion synchrotron at GSI were injected through several mm of diamond into solid samples pressurized up to 14 GPa in a diamond anvil cell. In synthetic graphite and natural zircon, the combination of pressure and ion beams triggered drastic structural changes not caused by the applied pressure or the ions alone. The modifications comprise long-range amorphization of graphite rather than individual track formation, and in the case of zircon the decomposition into nanocrystals and nucleation of the high-pressure phase reidite.

DOI: 10.1103/PhysRevLett.96.195701

PACS numbers: 61.80.Jh, 07.35.+k, 62.50.+p, 81.30.Hd

High-pressure and high-temperature experiments have aimed at reproducing the extreme conditions of the Earth's interior in order to better understand the material properties and quantify geodynamic processes [1–3]. In materials science, high pressure and temperature became important for manufacturing novel substances with, e.g., particular electrical, magnetic, or mechanical characteristics [4–8].

Alterations in solids, induced by heavy ions with primary kinetic energies up to several GeV, have been studied in great detail (see, e.g., [9]). One of the most crucial parameters is the energy loss per unit path length ( $dE/dx$ ) of the projectiles. The rapid and intense energy transfer to the target electrons excites and ionizes atoms along the ion path. Via electron-phonon coupling, most of the energy is finally transferred to the lattice. Especially in insulators, this leads to formation of tracks, cylindrical damage trails around the ion trajectories, with diameters of order 10 nm and macroscopic lengths (given by the ion energy) between a few  $\mu\text{m}$  and several mm. Track formation typically occurs above a critical material-dependent  $dE/dx$  threshold [10]. Examples of material modifications are crystalline-to-amorphous-phase [11] or superconductor-to-insulator [12] transformations, creation of a high-temperature [13] or high-pressure phase [14], generation of defect clusters [15], enormous irreversible deformations [16,17], and elastic inclusions [18]. For the mechanism of ion track creation, different models such as Coulomb explosion and thermal spike have been proposed [19,20].

Though there exists a large body of ion track data, almost no experimental information was available up to now [18], of how a solid copes with the simultaneous exposure to high pressure and energetic heavy ions: Can

such ions drive a pressurized material into a high-pressure phase? Two experimental conditions are indispensable for such investigations: (1) The sample must be enclosed in a high-pressure cell, and (2) the ions require sufficient kinetic energy to travel completely through one of the pressure anvils to reach and traverse the sample.

Here we report first experiments where pressure-exposed samples of synthetic, highly oriented pyrolytic graphite (HOPG) and of natural single-crystalline zircon ( $\text{ZrSiO}_4$ ) [21] were irradiated with swift heavy ions. We chose HOPG and zircon because a considerable amount of data from ion irradiation of nonpressurized samples is available for both materials. An additional reason was that the graphite/diamond transition is an example for a time-consuming reconstructive phase transformation, whereas the zircon/reidite transition represents a fast displacive high-pressure transformation to a scheelite-structured polymorph. Furthermore, radiation damage of zircon is of particular interest in geoscience and with respect to the possible application of this material for nuclear waste storage [22]. Prior to ion beam exposure, the zircon samples were annealed at 700 °C (24 hours) to eliminate preexisting natural damage such as dislocations and tracks from fission and  $\alpha$ -recoil nuclei.

Using diamond anvil cells (DAC) of the Merrill-Bassett type [23], we applied pressures up to 14 GPa. A 4:1 mixture of methanol and ethanol served as pressure transmitting medium, and the pressure was measured via ruby fluorescence [24]. Subsequently, we exposed the pressurized samples at room temperature (RT) to a beam of either  $^{238}\text{U}$  or  $^{197}\text{Au}$  ions accelerated to relativistic energies up to 70 GeV by the SIS heavy-ion synchrotron of GSI (see

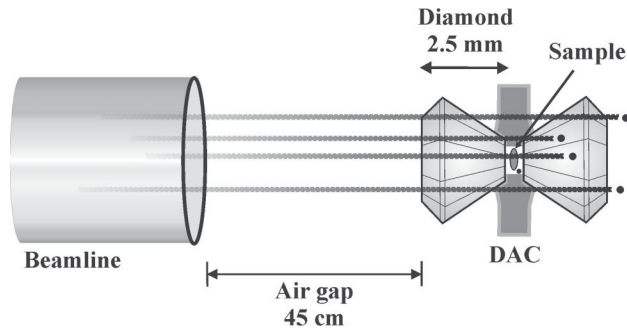


FIG. 1. Experimental scheme for the irradiation of pressurized samples with relativistic heavy ions (not to scale). The sample inserted in the diamond anvil cell is about  $100\ \mu\text{m}$  in diameter and  $50\ \mu\text{m}$  thick.

Fig. 1). The initial beam energy was chosen such that the energy loss inside the sample was for both materials above the experimentally known track formation thresholds [10,25]. We used a parallel pulsed beam (pulse width  $>50\ \text{ms}$ , rate  $\sim 1\ \text{Hz}$ ) of flux  $\sim 10^8\ \text{ions/s/cm}^2$ , low enough to avoid sample heating. The fluence applied was between  $2 \times 10^9$  and  $2 \times 10^{11}\ \text{ions/cm}^2$ , i.e., well below the onset of substantial track overlapping. Under ion irradiation, the diamond anvils emitted intense bluish-white luminescence; ion-induced coloration of the diamonds was not observed. The DAC pressure proved to be the same before and after irradiation, indicating that the diamond (known for its property not to record ion tracks) did not undergo any radiation damage impairing its functioning. The pressure was released instantaneously when opening the DACs after irradiation. As reference, HOPG and zircon were also irradiated without external pressure, i.e., outside the DAC using  $^{238}\text{U}$  ions of 2.6 GeV from the UNILAC linear accelerator of GSI. Details of essential irradiation parameters are summarized in Table I.

The samples were analyzed with transmission electron microscopy (TEM) in preexisting thin edge regions without further thinning to avoid any change or destruction of ion-induced features. Irradiated either without or under a low external pressure of 0.5 GPa, HOPG exhibited in both cases clearly defined ion tracks with an amorphous core of

about 20 nm in diameter, embedded in the well-ordered crystalline matrix and surrounded by a strain halo [Fig. 2(a)]. These findings are comparable with previous results obtained by scanning tunneling microscopy on HOPG irradiated without external pressure [10]. The smaller track size reported was probably due to the use of bulk rather than microscopic samples.

After irradiation at 8.4 and 12.1 GPa, TEM did not find any individual ion tracks but revealed a spatially extended conversion of HOPG into the amorphous state, interfused by bands of layered crystalline graphite with random orientations [Fig. 2(b)]. These nanocrystalline flakes are interconnected in the form of a turbostratic-like texture. Electron diffraction of the nonpressurized sample created the characteristic diffraction pattern of crystalline graphite, whereas the sample irradiated at 8.4 GPa produced several rings and spots resulting from randomly oriented graphite crystallites, and a diffuse background due to an amorphous matrix [see inset of Fig. 2(b)].

At RT, without pressure and also at 0.5 GPa, graphite is the thermodynamically stable form of carbon. On the other hand, graphite is, at 8.4 and 12.1 GPa, in the stability field of diamond but does not undergo any structural alterations in this pressure range [27,28]. While exposing our samples to 8.4 and 12.1 GPa, also the ions were not able to trigger a transformation to stable diamond. The absence of diamond in our high-pressure irradiations can be attributed to the sluggish kinetics of the phase transformation, preventing the formation of the stable phase [28]. However, the ions induced a long-range amorphization that represents a very different change compared with nanometer-sized tracks formed without pressure or at 0.5 GPa. In addition, we want to emphasize that this spatially extended damage occurred at  $dE/dx$  values that were significantly smaller than for the nonpressurized and 0.5 GPa samples (see Table I), underlining the pressure influence.

Also zircon exhibited novel effects when irradiated at 14.2 GPa with  $^{238}\text{U}$  ions ( $2 \times 10^9\ \text{ions/cm}^2$ ). At 14.2 GPa and RT, natural zircon is, according to [29], in the stability field of reidite, the high-pressure polymorph of  $\text{ZrSiO}_4$ . At RT, a transition to reidite is known to occur only for

TABLE I. Experimental details of the irradiation experiments.  $E_i$  and  $E_f$  denote the initial kinetic ion energy and the energy behind the first diamond anvil, respectively. The values were calculated with the SRIM code [26] by inserting the stopping power and thickness of the different in-beam components (exit window, air gap, anvil). Within the SRIM uncertainties of up to 15%, the results were confirmed by test experiments [25].

Material	Pressure [GPa]	Ion	Fluence [ $\text{ions/cm}^2$ ]	$E_i$ [GeV]	$E_f$ [GeV]	$dE/dx$ [keV/nm]
Graphite <sup>a</sup>	no	$^{238}\text{U}$	$1.0 \times 10^{11}$	2.6	2.6	27.0
Graphite	0.5	$^{238}\text{U}$	$1.9 \times 10^{11}$	44.7	17.1	13.0
Graphite	8.4	$^{238}\text{U}$	$1.0 \times 10^{11}$	68.3	40.5	8.0
Graphite	12.1	$^{197}\text{Au}$	$1.0 \times 10^{11}$	42.2	19.7	8.3
Zircon <sup>a</sup>	no	$^{238}\text{U}$	up to $8 \times 10^{12}$	2.6	2.6	43.0
Zircon	14.2	$^{238}\text{U}$	$2.0 \times 10^9$	47.6	13.8	24.5

<sup>a</sup>Irradiations performed in vacuum chamber at UNILAC (no diamond anvil involved).

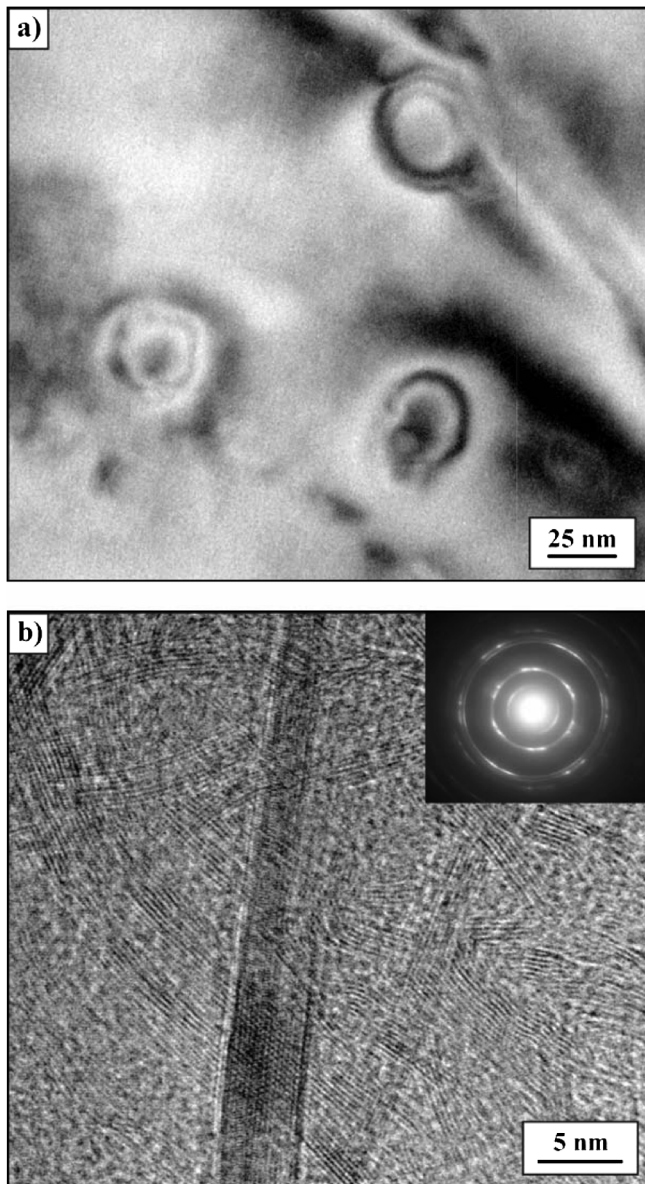


FIG. 2. TEM images of HOPG irradiated with about  $10^{11}$  uranium ions/cm<sup>2</sup> in a DAC at (a) 0.5 and (b) 8.4 GPa. The *c* axis is in both cases normal to the image plane and parallel to the ion trajectories. Micrograph (a) shows ion tracks consisting of an amorphous core and being surrounded by a strain halo within the otherwise undisturbed material. Image (b) displays an extended amorphous zone containing recrystallized graphite flakes with random lattice orientations. The phase change is supported by the electron diffraction pattern (inset).

pressures around or above 23 GPa [30] (for synthetic zircon, this transition occurs at a lower pressure of  $\sim 20$  GPa [31]). Our energetic ions, however, triggered the creation of this phase already at a pressure as low as 14.2 GPa. This was evidenced by Raman spectroscopy (after taking the sample out of the DAC) revealing bands of reidite [30–32] (Fig. 3). In contrast to this, after irradiating zircon without external pressure at the UNILAC, we

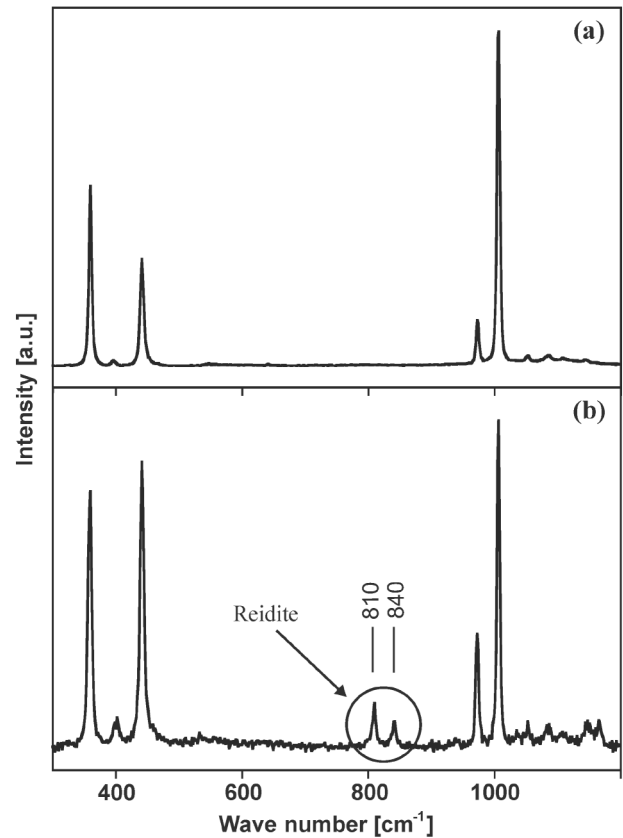


FIG. 3. Raman spectra of zircon (a) before and (b) after irradiation with  $2 \times 10^9$  uranium ions/cm<sup>2</sup> at 14.2 GPa, revealing new bands (810 and 840 cm<sup>-1</sup>) of the high-pressure polymorph reidite.

did not find any reidite bands even up to a fluence of  $8 \times 10^{12}$  uranium ions/cm<sup>2</sup>. Furthermore, TEM of the high-pressure sample visualized a composite of zircon and randomly oriented reidite crystallites with sizes of several nm (Fig. 4). We did not detect any individual amorphized ion tracks, as found in nonpressurized zircon [33–35].

In summary, our results demonstrate that the simultaneous exposure to high pressure and to ion beams triggers drastic structural changes in synthetic graphite and natural zircon not inducible by the applied pressure or the ions alone. Our TEM observations reveal that the combination of high pressure and a large amount of energy, deposited by swift heavy ions, stimulates alterations reaching far outside the ion trajectories, but does not create individual tracks. These modifications, comprising long-range amorphization of graphite, and decomposition of zircon into nanocrystals and nucleation of its high-pressure phase reidite, are possibly generated by pressure-pulse propagation [14,32,36].

We finally remark that the energy loss of the ions that we employed in the zircon experiment and the energy loss of nuclear fragments, generated by spontaneous fission, in natural minerals, are of similar size. Therefore, our results

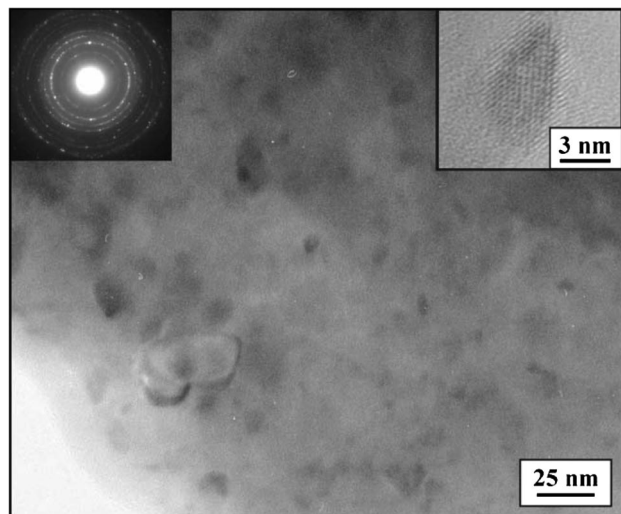


FIG. 4. TEM image of zircon after irradiation with  $2 \times 10^9$  uranium ions/cm<sup>2</sup> at 14.2 GPa. The ions induced a conversion of the pressurized zircon sample into an aggregate of zircon and reidite nanocrystals, several nm in size. The right inset shows a reidite nanocrystal, the left inset represents the characteristic electron diffraction pattern of reidite.

may also shed new light on the formation of reidite in nature.

The authors gratefully acknowledge technical support by Andreas Audéat, Johannes Baier, Bernd Binder, and Michael Dorn of the University of Tübingen, Germany, and by Gerhard Brey and Axel Gerdes of the University of Frankfurt/Main, Germany. This work was supported by the German Federal Ministry of Education and Research (Grant to G. A. W. and U. A. G.), and the German Science Foundation (Grant to U. A. G., Leibniz Grant to H. K.).

\*Present address: Geologisch-Paläontologisches Institut, Ruprecht-Karls Universität Heidelberg, Neuenheimer Feld 234, 69120 Heidelberg, Germany.

†Corresponding author.

Electronic address: ua.glasmacher@mpi-hd.mpg.de

- [1] R. Jeanloz, *Annu. Rev. Earth Planet. Sci.* **18**, 357 (1990).
- [2] E. Knittle and R. Jeanloz, *Science* **252**, 1438 (1991).
- [3] R. J. Hemley, *Annu. Rev. Phys. Chem.* **51**, 763 (2000).
- [4] E. Knittle, R. B. Kaner, R. Jeanloz, and M. L. Cohen, *Phys. Rev. B* **51**, 12 149 (1995).
- [5] R. J. Hemley and N. W. Ashcroft, *Phys. Today* **51**, No. 8, 26 (1998).
- [6] M. I. Erements, V. V. Struzhkin, H. K. Mao, and R. J. Hemley, *Science* **293**, 272 (2001).
- [7] K. Shimizu, T. Kimura, S. Furomoto, K. Takeda, K. Kon-tani, Y. Onuki, and K. Amaya, *Nature (London)* **412**, 316 (2001).
- [8] P. F. McMillan, *Nat. Mater.* **1**, 19 (2002).
- [9] *Nucl. Instrum. Methods Phys. Res., Sect. B* **245**, 1 (2006).

- [10] J. Liu, R. Neumann, C. Trautmann, and C. Müller, *Phys. Rev. B* **64**, 184115 (2001).
- [11] A. Meftah, F. Brisard, J. M. Costantini, E. Dooryhee, M. Hage-Ali, M. Hervieu, J. P. Stoquert, F. Studer, and M. Toulemonde, *Phys. Rev. B* **49**, 12 457 (1994).
- [12] H. Walter, W. Prusseit, R. Semerad, H. Kinder, W. Assmann, H. Huber, H. Burkhardt, D. Rainer, and J. A. Sauls, *Phys. Rev. Lett.* **80**, 3598 (1998).
- [13] W. Assmann, M. Dobler, D. K. Avasthi, S. Kruijjer, H. D. Mieskes, and H. Nolte, *Nucl. Instrum. Methods Phys. Res., Sect. B* **146**, 271 (1998).
- [14] H. Dammak, A. Barbu, A. Dunlop, D. Lesueur, and N. Lorenzelli, *Philos. Mag. Lett.* **67**, 253 (1993).
- [15] K. Schwartz, C. Trautmann, and R. Neumann, *Nucl. Instrum. Methods Phys. Res., Sect. B* **209**, 73 (2003).
- [16] S. Klaumünzer, L. Changlin, S. Löffler, M. Rammensee, and G. Schumacher, *Nucl. Instrum. Methods Phys. Res., Sect. B* **39**, 665 (1989).
- [17] A. Hedler, S. Klaumünzer, and W. Wesch, *Nat. Mater.* **3**, 804 (2004).
- [18] C. Trautmann, S. Klaumünzer, and H. Trinkaus, *Phys. Rev. Lett.* **85**, 3648 (2000).
- [19] H. Trinkaus and A. I. Ryazanov, *Phys. Rev. Lett.* **74**, 5072 (1995).
- [20] M. Toulemonde, Ch. Dufour, A. Meftah, and E. Paumier, *Nucl. Instrum. Methods Phys. Res., Sect. B* **166–167**, 903 (2000).
- [21] The HOPG was purchased from Advanced Ceramics Corporation, USA. The zircon samples, originating from Beaune-sur-Arzon, France, contain the following major impurities (in ppm): Hf (9087), Y (977), Yb (352), Ca (304), Er (152), P (79), Th (79), Fe (55), and U (50).
- [22] R. C. Ewing, *Can. Mineral.* **39**, 697 (2001).
- [23] L. Merrill and W. A. Bassett, *Rev. Sci. Instrum.* **45**, 290 (1974).
- [24] H.-K. Mao, J. Xu, and P. M. Bell, *Geophys. Res.* **91**, 4673 (1986).
- [25] M. Lang, U. A. Glasmacher, R. Neumann, C. Trautmann, D. Schardt, and G. A. Wagner, *Appl. Phys. A* **80**, 691 (2005).
- [26] <http://www.srim.org/SRIM/SRIM2003.htm>.
- [27] F. P. Bundy, W. A. Bassett, M. S. Weathers, R. J. Hemley, H.-K. Mao, and A. F. Goncharov, *Carbon* **34**, 141 (1996).
- [28] W. L. Mao, H. Mao, P. J. Eng, T. P. Trainor, M. Newville, C. Kao, D. L. Heinz, J. Shu, Y. Meng, and R. J. Hemley, *Science* **302**, 425 (2003).
- [29] S. Ono, K. Funakoshi, Y. Nakajima, Y. Tange, and T. Katsura, *Contrib. Mineral. Petrol.* **147**, 505 (2004).
- [30] E. Knittle and Q. Williams, *Am. Mineral.* **78**, 245 (1993).
- [31] W. van Westrenen, M. R. Frank, J. M. Hanchar, Y. Fei, R. J. Finch, and C.-S. Zha, *Am. Mineral.* **89**, 197 (2004).
- [32] A. Gucsik, M. Zhang, C. Koeberl, E. K. H. Salje, S. A. T. Redfern, and J. M. Pruneda, *Mineral. Mag.* **68**, 801 (2004).
- [33] K. Yada, T. Tanji, and I. Sunagawa, *Phys. Chem. Miner.* **14**, 197 (1987).
- [34] L. A. Bursill and G. Braunschhausen, *Philos. Mag. A* **62**, 395 (1990).
- [35] A. Meldrum, S. J. Zinkle, L. A. Boatner, and R. C. Ewing, *Phys. Rev. B* **59**, 3981 (1999).
- [36] D. Fenyő and R. E. Johnson, *Phys. Rev. B* **46**, 5090 (1992).